In Vitro Characterization of a Bacterial Manganese Uptake Regulator of the Fur Superfamily†

Pierdomenico Bellini and Andrew M. Hemmings*

Centre for Metalloprotein Spectroscopy and Biology, School of Chemical Sciences and Pharmacy and School of Biological Sciences, University of East Anglia, Norwich NR4 7TJ, United Kingdom

Received October 12, 2005; Revised Manuscript Received December 22, 2005

ABSTRACT: Fur proteins generally act as negative transcriptional regulators by binding to target regulatory sequences (*fur* boxes) in the promoter regions of iron-responsive genes. Recently, *Rhizobium leguminosarum* was reported to contain a protein (Mur_{Rl}) of Fur-like sequence, which, under manganese-replete conditions in its native background, repressed transcription of an ABC-type Mn(II) transporter by binding to two nonpalindromic *mur* boxes in its promoter region. Mur_{Rl} displays apparently unusual regulatory flexibility in that it can also repress iron-responsive genes in *Escherichia coli* under iron-replete conditions. In this study, we quantify the affinities for binding a number of first-row transition-metal cations by Mur_{Rl} and demonstrate that, in a fashion similar to *E. coli* Fur, Mur_{Rl} binds Mn(II), Fe(II), Zn(II), and Co(II) with similar micromolar-order dissociation constants. In contrast to the vast majority of Fur proteins, however, Mur_{Rl} lacks any high-affinity structural Zn(II) sites. Furthermore, we show that holoMur_{Rl} binds as one and two homodimers to both *mur* and *fur* boxes in a concentration-dependent fashion in the presence of not only Mn(II) and Fe(II) but also Zn(II) and Co(II). We have developed an analytical method for determination of the individual dissociation constants and find that the DNA-binding affinities are essentially independent of the metal co-effector. These results complement those obtained *in vivo* by other authors and suggest that the Fur-like protein of *R. leguminosarum*, a competent ferric uptake regulator in *E. coli*, is insufficiently discriminating in its metal-binding characteristics to function as a regulator of iron homeostasis in its native background.

Classically, the ferric uptake regulator (Fur) protein has been viewed as a global iron-responsive negative transcriptional regulator of a wide range of genes in bacteria, many of which encode the biosynthesis and uptake of siderophores (*1*). The currently accepted view is more complex, acknowledging that Fur is also involved in the regulation of a range of other iron metabolism-related processes and also in processes not obviously related to iron (*2*). A growing number of Fur superfamily proteins have been identified with Fur orthologues found in many Gram-negative bacteria and also some low GC-content Gram-positive bacteria. These are proteins with Fur-like sequences but which recognize different corepressors and carry out a variety of regulatory roles. The zinc-uptake regulator, Zur, which responds to Zn(II), was first described in *Bacillus subtilis* (*3*) and *Escherichia coli* (*4*) where it represses the transcription of genes encoding a zinc ABC (ATP-binding cassette) transport system. Subsequently, Zur proteins have been identified in other bacteria such as *L. monocytogenes* (*5*). PerR, the peroxide response regulator, regulates oxidative response genes in *B. subtilis*, *Campylobacter jejuni*, *Staphylococcus aureus*, and *Streptococcus pyogenes* (*6*−*9*). PerR from *B. subtilis* has also been shown to respond to Fe(II) or Mn(II) depending upon the particular promoter (*10*). Irr, the iron-responsive regulator, is another Fur-like protein first identified in *Bradyrhizobium japonicum* (*11*), which, under Fe-deplete conditions, represses *hemB*, a gene involved in heam biosynthesis. Under Fe-replete conditions, Irr is targeted for degradation via a post-translational pathway (*12*). Notably, the Irr family may be the most divergent among the Fur superfamily group in that its members are active in the absence of metal rather than its presence.

The final Fur family characterized to date involves proteins involved in the regulation of bacterial manganese uptake. Fur or Fur-like proteins are involved in the regulation of ABC-type Mn(II) permeases in a number of bacteria including *Yersinia pestis* and *Salmonella enterica* (*13*, *14*). Recently, two further examples have been described from the α proteobacteria, *Rhizobium leguminosarum* (*15*) and *Sinorhizobium meliloti* (*16*). The manganese uptake regulator of *R. leguminosarum* (Mur_{Rl}) is a cytoplasmic protein, which, under manganese-replete conditions, represses transcription of the *sitABCD* operon, which specifies a Mn(II) transporter of the ABC class (*15*). Interestingly, repression was not observed in conditions of excess Fe(II). The amino acid sequence of Mur_{Rl} is 38% identical to both *E. coli* Fur (Fur_{Ec}) and the Fur from *Pseudomonas aeruginosa* (Fur_{Pa}). No consensus *fur* boxes occur in the promoter regions of iron-responsive genes in *R. leguminosarum* nor is the expression of a number of such operons affected by the *mur* mutation

† This work was supported through the award of a University of East Anglia Ph.D. Studentship to P.B.

* To whom correspondence should be addressed: School of Biological Sciences, University of East Anglia, Norwich NR4 7TJ, U.K. Telephone: +44-(0)1603-592777. Fax: +44-(0)1603-592250. E-mail: a.hemmings@uea.ac.uk.

10.1021/bi052081n CCC: $33.50
Published on Web 02/03/2006

(*17*). Indeed, no further proteins with a Fur-like sequence are predicted from the analysis of the *R. leguminosarum* genome, and the iron-sensing role of Fur in this organism is taken by a recently discovered regulator, RirA (*18*), a protein showing no sequence homology with Fur proteins. Conversely, under iron-replete conditions, Mur_{Rl} is able to correct an *E. coli fur* deletion mutant and represses a promoter (*bfd*) that is recognized by Fur_{Ec} (*17*). Also, in the presence of excess Mn(II), Mur_{Rl} can retard a DNA fragment *in vitro* containing the archetypal *fur* box preceding *pvdS* of *P. aeruginosa* (*17*) [note that Mn(II) is a commonly adopted surrogate corepressor used in studies of Fur activity]. In addition, Mur_{Rl} shares a high degree of sequence identity (65%) with the Fur protein of *B. japonicum*, Fur_{Bj}, which in turn shares 38% identity with Fur_{Ec}. Fur_{Bj} has been shown to bind to a *fur* box in the *irr* promoter region and can complement an *E. coli fur* deletion mutant (*19*). When these observations are taken together, they support the emerging view that the mechanisms for the regulation of iron uptake in the rhizobia are very different from those in the γ proteobacteria, such as *E. coli* (*18*, *20*).

fur, *zur*, *perR*, *irr*, or *mur* boxes are usually found to be palindromic and 19 or 21 bp long, depending upon interpretation. The canonical *fur* box can be viewed as either a 9−1−9 palindrome (*21*), as three imperfect direct repeat pentamers with the sequence AT/^{A}/$_{T}$/AT (*22*), as two direct and one inverted hexamer with the sequence GATAAT (*22*), or as two overlapping 7−1−7 inverted repeats (*23*). In addition, Friedman and O'Brian (*19*) have shown by DNase I footprinting analysis that Fur_{Bj} maximally protects a 30-bp region of the *irr* promoter region containing a noncanonical *fur* box that can be interpreted as three imperfect direct repeat hexamers. In the presence of Mn(II) as a surrogate corepressor, one and two Fur_{Bj} dimers were shown to bind to either a canonical (palindromic) *fur* box consensus sequence or to the dsDNA sequence in the *B. japonicum irr* promoter region at low and high concentrations, respectively, whereas Fur_{Ec} only recognized the *fur* box (*19*). Electrophoretic mobility shift assays involving the complete *sitABCD* promoter region of *R. leguminosarum* led to the proposal that Mur_{Rl} recognizes two 21-bp sequences, Mur responsive sequences 1 and 2 (labeled *mrs1* and *mrs2*, respectively) spaced 34 bp apart in the *sitABCD* promoter region. These bear only superficial similarity to the canonical *fur* box sequence and are only partially palindromic (*15*) (Figure 1).

The only crystal structure of a Fur superfamily protein available to date is that of holo Zn(II)-Fur_{Pa} (*24*). The protein folds to give a C-terminal α/β dimerization domain and two N-terminal helix−turn−helix motif-containing DNA-binding domains (one from each monomer). The Fur_{Pa} structure contains two Zn(II) ions per monomer: one binding site (labeled S1) lying within the C-terminal domain and the other (labeled S2) located at the interface between the C- and N-terminal domains. X-ray absorption spectroscopy and microPIXE analysis of Fe(II)-treated Fur_{Pa} in solution showed S2 to be occupied by Zn(II) and S1 by Fe(II) (the latter presumably replaced by zinc in the crystal structure because of its high concentration used during crystallization) (*24*). Therefore, the two binding sites S1 and S2 of Fur_{Pa} were inferred by the authors as corresponding to sensing and structural sites, respectively. All of the ligands contributing

```
                    **  *   *     *    **
fur box       5′- TGATAATGATAATCATTATCA -3′
              3′- ACTATTACTATTAGTAATAGT -5′

mrs1          5′- TGCAATTCATTCTTAATTGCA -3′
              3′- ACGTTAAGTAAGAATTAACGT -5′

mrs2          5′- TGCAAATCATTCTGAATCGCA -3′
              3′- ACGTTTAGTAAGACTTAGCGT -5′

irr promoter  5′- TGCGAGAAACTTGCATCTGCA -3′
              3′- ACGCTCTTTGAACGTAGACGT -5′
```

FIGURE 1: Comparison of the core regulatory sequences of different Fur superfamily proteins. A pseudopalindromic canonical *fur* box (*21*), *mrs1* and *mrs2* from *R. leguminosarum* (*15*), and the noncanonical *fur* box from *B. japonicum* (*19*) are shown. Bases corresponding to potential overlapping $(7-1-7)_2$ inverted repeats (*23*) are shown in bold. Conserved bases are indicated by an asterisk.

to metal-binding sites S1 and S2 in Fur_{Pa} are conserved in the sequences of Mur_{Rl}, Fur_{Ec}, Fur_{Bj}, and *Vibrio anguillarum* Fur (Fur_{Va}) (Figure 2). Surprisingly, however, mutants of Fur_{Bj} containing alanine substitutions in the corresponding binding sites S1 or S2 retained high DNA-binding affinity and repressed transcription *in vitro* in an Fe(II)-dependent manner (*25*). Thus, in *B. japonicum* Fur at least, binding of a structural metal may not be necessary a prerequisite for activity. Fur_{Ec} and Fur_{Va} have an additional very tightly bound zinc ion per monomer removable by ethylenediaminetetraacetic acid (EDTA)[1] treatment only after denaturation of the protein (*26*, *27*). This site is not present in Fur_{Pa} (*28*). Two of the four ligands of this tightly bound Zn(II) ion have been identified as cysteines (*26*) that are only conserved in Fur_{Ec} and Fur_{Va} (Figure 2). For present purposes, we may label this additional structural site S3 and note that the residues involved in providing ligands to the S3 zinc ion are not conserved in the rhizobial Fur_{Bj} or Mur_{Rl} proteins.

When the available *in vivo* data are taken together, they suggests that in *R. leguminosarum* Mur_{Rl} binds to *mur* boxes and represses transcription in response to manganese but not iron yet binds to canonical *fur* boxes and represses transcription in response to iron but not to manganese in *E. coli fur* deletion mutants (*15*). We were therefore interested to probe the apparently unusual metal- and DNA-binding specificity of the protein. In the present study, we report the first *in vitro* characterization of a manganese uptake regulator of the Fur superfamily, Mur_{Rl}. We demonstrate the surprising result that Mur_{Rl} binds a range of divalent transition-metal cations at a molar ratio of one ion per protein monomer, and this alone is apparently sufficient to result in high-affinity binding to both *mur* and *fur* boxes. We develop an analytical method for determination of the cooperativity in binding a ligand to a bivalent receptor and use it to investigate the affinity of Mur_{Rl} *in vitro* for both its cognate regulatory sequences and for canonical and noncanonical *fur* boxes. We discuss our results in terms of the growing body of data that supports the view that Fur superfamily proteins from different

[1] Abbreviations: CD, circular dichroism; DTT, dithiothreitol; EDTA, ethylenediaminetetraacetic acid; EMSA, electrophoretic mobility shift assay; HMC, high-mobility complex; ICP-AES, inductively coupled plasma atomic emission spectroscopy; ITC, isothermal titration calorimetry; ONPG, *o*-nitrophenyl-β-D-galactopyranoside; LMC, low-mobility complex.

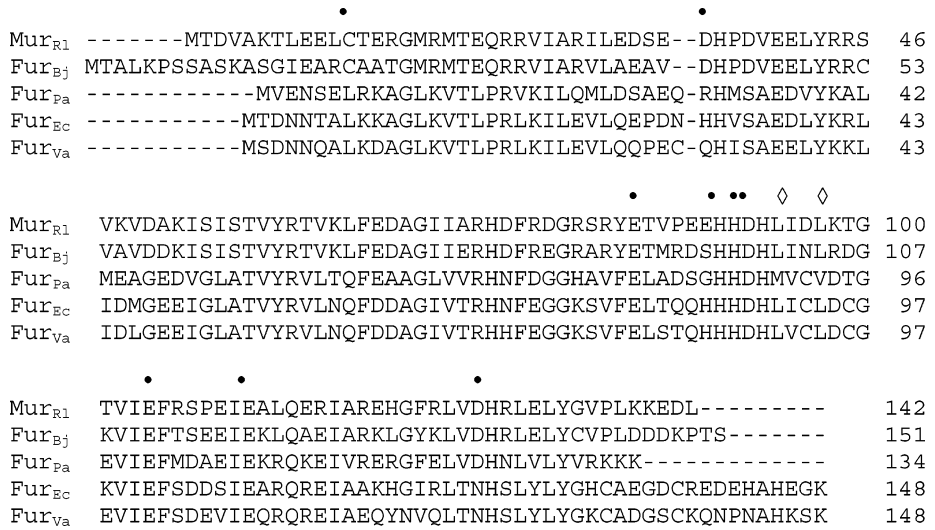

FIGURE 2: Primary sequence alignment generated using T-COFFEE (*38*) of selected proteins belonging to the Fur superfamily. Sequences shown are those from *R. leguminosarum* (Mur_{Rl}), *B. japonicum* (Fur_{Bj}), *P. aeruginosa* (Fur_{Pa}), *E. coli* K12 (Fur_{Ec}), and *V. anguillarum* (Fur_{Va}). ● and ○, respectively, represent residues in the putative sensing Fe(II)-binding site (S1) and the structural Zn(II)-binding site (S2) of *P. aeruginosa* Fur (*24*). The sole cysteine of Mur_{Rl} at position 12 is usually substituted by a leucine in Fur-like proteins. ◇ represents the two cysteines involved in the S3 site of Fur_{Ec} and Fur_{Va}, a very high-affinity structural Zn(II) site.

genera function in a complex background of processes contributing to metal homeostasis.

EXPERIMENTAL PROCEDURES

Chemicals and Reagents. All chemicals were reagent-grade and were purchased from Sigma and Fisher. Agar and yeast extract were purchased from Roche.

Bacterial Strains, Plasmids, Media, and Growth. E. coli strain DH5α was used for the propagation of plasmids and was grown on Luria−Bertani (LB) media with appropriate antibiotics. Plasmid pMur, a pET21a-based vector (Novagen), contained the *R. leguminosarum mur* gene derived from the wild-type strain, cloned into the *Nde*I and *Xho*I restriction sites. A stop codon was introduced at the *Xho*I site to allow for the expression of the native protein (Mur_{Rl}) without a His tag at the C terminus.

Overexpression, Purification, and Demetalation of Mur_{Rl}. Mur_{Rl} was overexpressed in *E. coli* strain BL21 (DE3) transformed with pMur and initially grown in 5 mL of LB media containing ampicillin (100 μg/mL). A total of 1 mL of culture from an overnight growth was used to inoculate 1 L of LB media again containing 100 μg/mL ampicillin. Overexpression was induced in cells at mid-log phase by adding a final concentration of 0.4 mM isopropyl-1-thio-β-D-galactopyranoside, and cells were left growing at 37 °C for another 4 h with shaking. Cells were harvested by centrifugation at 4000*g* for 10 min at 4 °C using a Becknam Avanti J-20 centrifuge. The pellet was resuspended in 10 mL of binding buffer (20 mM Tris-HCl at pH 7.5, 500 mM NaCl, and 10 mM imidazole), and the cells were sonicated using a Dawe Soniprobe for 2 min at 10 μm amplitude on ice. The cell debris was then centrifuged for a further 15 min at 45000*g*. The supernatant was syringe-filtered using 0.45 μm Sartorius filters and then poured into a 10 mL column containing IDA resin (Novagen) previously washed with 50 mM $NiCl_2$ and subsequently equilibrated with 10 column volumes (CVs) of binding buffer (this and all subsequent purification steps took place at 4 °C). The column was then washed with 15 CVs of wash buffer (20 mM Tris-HCl at pH 7.5, 500 mM NaCl, and 100 mM imidazole), and the protein was then eluted by applying elution buffer (20 mM Tris-HCl at pH 7.5, 500 mM NaCl, and 1 M imidazole). The whole process was run at 7 mL/min using a peristaltic pump (Amersham Biosciences). Elution fractions containing Mur_{Rl} were pooled and poured into a Hi-Load Superdex 75 gel-filtration column (Amersham Biosciences) equilibrated with 20 mM Tris-HCl at pH 7.5, 150 mM NaCl, and 5 mM EDTA. Gel-filtration fractions containing pure Mur_{Rl} as judged by SDS−PAGE were pooled and dialyzed against 5 L of reservoir buffer containing 20 mM Tris-HCl at pH 7.5 and 500 mM NaCl using a Spectra/Por membrane (Spectrum Laboratories) with a molecular-weight cut off (MWCO) of 3 kDa. Demetalation continued by dialysis of the sample against 5 L of reservoir buffer containing 20 mM Tris-HCl at pH 7.5 and 150 mM NaCl. Each dialysis step was carried out for at least 4 h using glassware that had been washed overnight in 10% HCl. All protein concentrations were determined using a Bradford assay (BioRad) and calibrated using spectrophotometric measurements employing a molar extinction coefficient of 5120 M^{-1} cm^{-1} at a wavelength of 280 nm.

Construction of a (C12A)Mur_{Rl} Mutant. Nucleotides in the cloned *mur* gene coding for residue cysteine 12 were altered to code for an alanine using QuikChange (Stratagene), producing the plasmid p(C12A)Mur. The mutation was verified by gene sequencing and electrospray ionization mass spectrometry of the protein. (C12A)Mur_{Rl} was overexpressed, purified, and demetalated as described for the wild-type protein. The secondary-structure content of the metal-free mutant protein was checked by a comparison of its far-UV circular dichroism (CD) spectra with that of apoMur_{Rl} using a π-180 CD spectropolarimeter (Applied Photophysics) calibrated with 0.1% (v/v) (+)-10-camphorsulfonic acid. Samples were buffer-exchanged by extensive dialysis to 20 mM sodium phosphate at pH 7.3, and the protein concentration was approximately 1 mg/mL (approximately 60 μM of monomer) in each case. Sample spectra were recorded at a path length of 2 mm from 195 to 260 nm at 22 °C. The step

resolution for all measurements was 0.2 nm with a speed of 100 nm/min. The response time was set to 0.5 s with a bandwidth of 1 nm and a sensitivity of 20 millidegrees. CD spectra were corrected for by subtraction of the spectrum in the presence of buffer alone. Secondary-structure content was then determined using CDNN (*29*). No significant difference was observed between the secondary-structure contents of apoMur_{Rl} and apo(C12A)Mur_{Rl} resulting from deconvolution, confirming the correct folding of the mutant. The observed secondary-structure content was α helix, 30%; β sheet, 21%; β turn, 17%; and coil, 34%.

Determination of the Protein Activity in Vivo Using a β-Galactosidase Assay. E. coli MC4100 transformed with p1459, a plasmid containing the *sitA* promoter-*lacZ* fusion, and either pMur or p(C12A)Mur were used to inoculate 10 mL of LB media with suitable antibiotic concentrations. Cultures were grown to a final cell density of approximately $2-5 \times 10^8$ mL^{-1} (corresponding to an OD_{600} of 0.28−0.70). A total of 0.5 mL of the culture was removed and placed in a 2 mL eppendorf tube and diluted to a final volume of 1 mL with Z buffer [100 mM phosphate buffer at pH 7.5, 10 mM KCl, 1 mM $MgSO_4$, and 0.5% (v/v) β-mercaptoethanol]. Three replicates for each strain were used in these studies. The cells were lysed by adding 50 μL of chloroform and 25 μL of 0.1% (w/v) SDS. Tubes were placed at room temperature for 5 min. A total of 0.2 mL of 4 mg/mL *o*-nitrophenyl-β-D-galactopyranoside (ONPG) was added to each sample and left at room temperature for 8 min. A total of 0.5 mL of 1 M Na_2CO_3 was then added to stop the reaction, and the tubes were spun down for 1 min at 5000*g* to remove cell debris. Supernatants were collected, and an OD_{420} was measured, using Z buffer to blank the spectrophotometer. β-Galactosidase activity was calculated in Miller units according to the formula:

$$\text{activity} = (1000 \times OD_{420})/(t \times v \times OD_{600})$$

where t is the time of sample incubation with ONPG and v is the volume of cell culture used for the assay.

Determination of Binding Affinities for Various Transition-Metal Cations Using Isothermal Titration Calorimetry (ITC). A total of 2.5 mL of previously degassed and demetalated (C12A)Mur_{Rl} protein at a monomer concentration of 18 μM was loaded into the cell of a Microcal isothermal titration calorimeter. Titrations of different metals [Mn(II), Fe(II), Zn-(II), Ni(II), and Co(II), with Ca(II) included as a negative control] were carried out by injecting 1 μL of 5 mM metal solution every 60 s. All titrations were continued until a 10-fold molar excess of metal ion over the monomer concentration was achieved. All of the metal solutions were prepared from divalent metal chlorides dissolved in water except for ferrous iron. The latter was freshly prepared in an anaerobic environment as an iron ammonium sulfate salt dissolved in a slightly acidic solution (pH 4.5 using HCl) to decrease the rate of oxidation. Experiments were carried out at 28 °C according to the instructions of the manufacturer. Data were analyzed by a version of Origin modified for ITC data analysis as supplied by Microcal. All experiments were carried out in triplicate.

Detection of Metal Binding by Atomic Emission Spectroscopy. A total of 5 mL of 5 μM (monomer concentration) demetalated (C12A)Mur_{Rl} protein samples was dialyzed overnight in 5 L of reservoir buffer (20 mM Tris-HCl at pH 7.5 and 100 mM NaCl) containing either 0.5 mM $MnCl_2$ or $ZnCl_2$ ($CaCl_2$ was also used as a negative control). The samples were then dialyzed overnight in 5 L of metal-free buffer (20 mM Tris-HCl at pH 7.5 and 100 mM NaCl) before being subjected to metal concentration analysis by atomic emission spectroscopy. The inductively coupled plasma atomic emission spectroscopy (ICP-AES) instrument used for these experiments was a Vista-PRO Simultaneous from Varian. The wavelengths used to detect the atomic emissions were 214, 258, and 423 nm for zinc, manganese, and calcium, respectively. The concentration of metal in the dialysis reservoir was also measured and subtracted from that of the protein sample. Measurements were taken from triplicate samples prepared with each metal. Using K_d values for metal binding measured by ITC, we then calculated the expected concentration of metal in each ICP-AES sample (for the method see the Supporting Information).

Electrophoretic Mobility Shift Assays (EMSAs). EMSA was performed as described by Ochsner et al. (*30*) with minor modifications. Four 27-bp DNA oligomers (supplied by MWG Biotech) labeled with fluorescein at the 5′ end were used: *mrs1* (5′-TGT TGC AAT TCA TTC TTA ATT GCA CAA-3′) and *mrs2* (5′-TTT TGC AAA TCA TTC TGA ATC GCA ACT-3′) found in the *R. leguminosarum sitABCD* promoter region (*15*); a canonical *fur* box consensus sequence flanked by three base pairs chosen to minimize possibilities of self-annealing (5′-TGT TGA TAA TGA TAA TCA TTA TCA CCC-3′); and the Fur_{Bj} box (5′-GTT GCG AGA AAC TTG CAT CTG CAT CTA-3′) in the promoter region of *B. japonicum irr* (*19*). The complementary oligomers for each were also fluorescein-labeled. A 27-bp oligomer based on a nonself-annealing, scrambled *fur* box sequence was also used as a negative control. Single-stranded DNA oligomers were annealed by mixing equal concentrations of DNA, followed by incubation at 90 °C for 10 min and subsequent slow cooling to room temperature.

For analysis of binding affinities, increasing concentrations of apoMur_{Rl} in the presence of 1 mM dithiothreitol (DTT) and a 5-fold excess of metal ions over the highest protein dimer concentration were employed. DNA concentrations used were 40 nM for *mrs1* and *mrs2* and 200 nM for the canonical *fur* box and Fur_{Bj} box. Assays were performed in the presence of Mn(II), Fe(II), Zn(II), and Co(II). Ca(II) was also employed as a negative control. For each of the DNA probes, a further control was performed by running the EMSA in the presence of a 5-fold excess of EDTA over the protein monomer concentration. The ferrous iron solution, prepared as described for ITC experiments, was preincubated with the protein−DNA sample in an anaerobic environment prior to rapid loading onto the gel. The remaining metals were simply incubated with the protein−DNA mixture for 15 min at 32 °C prior to electrophoresis. Metals were not present in either the running buffer or in the gel itself because of metal oxidation during gel settlement. Bands were visualized using a Molecular Imager FX (BioRad), and bound and unbound DNA was quantified by comparing relative signal intensities using Quantity One (BioRad). A further negative control experiment was carried out in each case.

Determination of the Molecular Weights of Mur_{Rl}−DNA Complexes. Ferguson plots were employed to estimate the molecular weights of Mur_{Rl}−DNA complexes. This proce-

dure was carried out as described by Friedman and O'Brian (*19*).

Detection of Cooperativity between Identical Binding Sites of a Bivalent Receptor through Determination of Macroscopic Dissociation Constants. Consider a receptor with two identical binding sites such as a palindromic dsDNA sequence with two overlapping binding elements (a canonical *fur* box) to which two proteins can bind. A ligand will first randomly occupy one of the two identical binding elements ($e_{1/2}$) of such a receptor and subsequently the other ($e_{2/1}$). Dependent upon the effect on the second binding element because of ligand binding to the first binding element, three possible scenarios can occur (1) the ligand binds to $e_{1/2}$ with a dissociation constant K_{d_1} and to $e_{2/1}$ with a dissociation constant K_{d_2}, with $K_{d_1} > K_{d_2}$ (positive cooperativity); (2) the ligand binds to $e_{1/2}$ with K_{d_1} and to $e_{2/1}$ with K_{d_2}, with $K_{d_1} < K_{d_2}$ (negative cooperativity); (3) the ligand binds to $e_{1/2}$ with a dissociation constant K_{d_1} and to $e_{2/1}$ with K_{d_2}, with $K_{d_1} = K_{d_2}$ (no cooperativity, which means that $e_{1/2}$ and $e_{2/1}$ are indistinguishable). The two dissociation constants K_{d_1} and K_{d_2}, according to the law of mass action, can be described as

$$K_{d_1} = \frac{(R - y_1)(L - y_1 - y_2)}{y_1} \tag{1}$$

and

$$K_{d_2} = \frac{(y_1 - y_2)(L - y_1 - y_2)}{y_2} \tag{2}$$

where R is the receptor concentration, L is the ligand concentration, y_1 [low-mobility complex (LMC) + high-mobility complex (HMC) in Figure 4] is the concentration of occupied $e_{1/2}$, and y_2 (LMC in Figure 4) is the concentration of occupied $e_{2/1}$. It is possible to extrapolate either y_1 or y_2 using both eqs 1 and 2 to create a combination of binding curves in L containing only the known quantity R (total amount of receptor) and the two unknown parameters K_{d_1} and K_{d_2}. These curves can then be fitted to experimental data plotted as fractions of either y_1 or y_2 against the ligand concentration to estimate the two unknown parameters K_{d_1} and K_{d_2}. The most convenient way to proceed is by rearranging eq 1 in terms of y_2 and then by substituting the result into eq 2 to obtain, after regrouping, a cubic equation for y_1

$$y_1^3 + a_2 y_1^2 + a_1 y_1 + a_0 = 0 \tag{3}$$

where

$$a_2 = \frac{K_{d_2} - K_{d_1} - 2RK_{d_1} - K_{d_1}^2}{2K_{d_1}} \tag{4}$$

$$a_1 = \frac{LRK_{d_1} - LK_{d_2} - K_{d_1}K_{d_2} - RK_{d_2}}{2K_{d_1}} \tag{5}$$

$$a_0 = \frac{LRK_{d_2}}{2K_{d_1}} \tag{6}$$

Standard methods used in binding analysis simplify the cubic eq 3 to a linear equation using the constriction that the ligand concentration can be assumed to be much greater than that of the receptor (*31*). Because the protein (ligand) concentration was not much greater than that of the DNA (receptor) in the EMSAs described above (because of the limitation in detection of fluorescein-labeled DNA), it was necessary to derive an unconstrained method to provide accurate quantitative analysis of the binding data. The three solutions y_{11}, y_{12}, and y_{13} for the cubic equation are given by the cubic formula (http://mathworld.wolfram.com/CubicFormula.html), and in this case, where the polynomial discriminant is less than 0, they are

$$y_{11} = 2\sqrt{-Q}\cos\left(\frac{\theta}{3}\right) - \frac{1}{3}a_2 \tag{7}$$

$$y_{12} = 2\sqrt{-Q}\cos\left(\frac{\theta + 2\pi}{3}\right) - \frac{1}{3}a_2 \tag{8}$$

$$y_{13} = 2\sqrt{-Q}\cos\left(\frac{\theta + 4\pi}{3}\right) - \frac{1}{3}a_2 \tag{9}$$

where

$$\theta = \cos^{-1}\left(\frac{P}{\sqrt{-Q^3}}\right) \tag{10}$$

$$Q = \frac{3a_1 - a_2^2}{9} \tag{11}$$

$$P = \frac{9a_1a_2 - 27a_0 - 2a_2^3}{54} \tag{12}$$

Solutions y_{11} and y_{12} do not make sense because eqs 7 and 8, respectively, increase and decrease indefinitely. The "real" solution is eq 9, which gives a "saturation curve". However, determination of K_{d_2} using eq 9 is prompt to significant errors even though the binding curve shows an excellent fit to the data. This is due to the fact that extrapolation of y_2 for substitution into eq 2 was originally derived from eq 1, where the contribution of y_2 is usually not significant until the ligand reaches a reasonably high concentration. Consequently, the contribution of K_{d_2} to eq 9 is also minimal with insignificant changes to the binding curve over a wide range of different values, which makes its correct determination difficult. Therefore, while eq 9 is useful to estimate K_{d_1}, it is not advisable to use it to estimate K_{d_2}. The contribution of y_2 and, consequently, K_{d_2} to the binding curve can be increased by creating a binding curve explicitly for y_2. The most convenient way to proceed in deriving an equation for y_2 that does not contain y_1 is by first rearranging eq 1 in terms of $(L - y_1 - y_2)$ and by substituting the result into eq 2, to obtain, after regrouping

$$\frac{K_{d_1}y_1}{R - y_1} = \frac{K_{d_2}y_2}{y_1 - y_2} \tag{13}$$

Rearranging then eq 13 in terms of y_2 and substituting eq 9 for y_1 gives

$$y_2 = \frac{K_{d_1}(y_{13})^2}{RK_{d_2} - K_{d_2}(y_{13}) + K_{d_1}(y_{13})} \tag{14}$$

where y_{13} is described in eq 9.

Binding curves for y_1 minus y_2 (HMC in Figure 4) as well as for the sum of y_1 and y_2 (2×LMC + HMC) can also be easily obtained by substituting eqs 9 and 14 for y_1 and y_2, respectively, to give

$$y_1 - y_2 = y_{13} - \frac{K_{d_1}(y_{13})^2}{RK_{d_2} - K_{d_2}(y_{13}) + K_{d_1}(y_{13})} \quad (15)$$

$$y_1 + y_2 = y_{13} + \frac{K_{d_1}(y_{13})^2}{RK_{d_2} - K_{d_2}(y_{13}) + K_{d_1}(y_{13})} \quad (16)$$

where y_{13} is described in eq 9. Note that, because y_1 plus y_2 is equivalent to HMC plus 2 times LMC, eq 16 has to be divided by twice R to obtain fractions of bound ligand. Eqs 14, 15, and 16 were observed to be equally efficacious for determination of both K_{d_1} and K_{d_2}. The method then provides accurate K_d values for both binding events and hence an indication of whether cooperativity in binding is operational.

Unconstrained Analysis of Ligand Binding to a Bivalent Receptor with Nonidentical Binding Sites. For the case of the Mur_{Rl} protein binding to nonpalindromic *mrs1*, *mrs2*, or *irr* box DNA, we have assumed the receptor to be bivalent with nonidentical binding sites. The following method will provide an estimation of macroscopic dissociation constants for both binding events. However, in this case, it is not possible to distinguish whether the difference between K_{d_1} and K_{d_2} is due to negative cooperativity or to differences in the structures of the binding sites (or to both of them).

In the case of a bivalent receptor with independent and nonidentical binding sites, the dissociation constant for ligand binding to a specific binding site, S1, can still be described by eq 1. However, the dissociation constant of the ligand binding to the other site, S2, is now described by

$$K_{d_2} = \frac{(R - y_2)(L - y_2 - y_1)}{y_2} \quad (17)$$

The fraction of bound ligand, B_L, assuming that the sites are independent, is then given by

$$B_L = \frac{y_1 + y_2}{2R} \quad (18)$$

y_1 can be derived by rearranging eq 1 in terms of y_2 and then by substituting the result into eq 17 to obtain, after regrouping, a cubic equation for y_1, where the real solution is again given by eq 9 and

$$a_2 = \frac{K_{d_2} - LK_{d_1} - K_{d_1}^2}{K_{d_1}} \quad (19)$$

$$a_1 = \frac{LRK_{d_1} - K_{d_1}K_{d_2} - LK_{d_2} - RK_{d_2} - R^2K_{d_1}}{K_{d_1}} \quad (20)$$

$$a_0 = \frac{LRK_{d_2}}{K_{d_1}} \quad (21)$$

Following the same principle, y_2 can be derived by rearranging eq 17 in terms of y_1 and then by substituting the result into eq 1 to obtain, after regrouping, a cubic equation for y_2, where the real solution is also given by eq 9 and

$$a_2 = \frac{K_{d_1} - LK_{d_2} - K_{d_2}^2}{K_{d_2}} \quad (22)$$

$$a_1 = \frac{LRK_{d_2} - K_{d_2}K_{d_1} - LK_{d_1} - RK_{d_1} - R^2K_{d_2}}{K_{d_2}} \quad (23)$$

$$a_0 = \frac{LRK_{d_1}}{K_{d_2}} \quad (24)$$

Table 1: β-Galactosidase Activities Directed by a Plasmid-borne *SitA-lacZ* Fusion in Δ Transformed with Plasmids Expressing Mur_{Rl} and (C12A)Mur_{Rl}

sample	activity (Miller units) +Mn(II)	activity (Miller units) +bipyridyl
MC4100 (*E. coli* strain *lacZ*$^-$)	31 ± 1	35 ± 3
MC4100 + *SitA-lacZ* fusion	165 ± 27	178 ± 31
MC4100 + *SitA-lacZ* fusion + Mur_{Rl}	41 ± 12	145 ± 25
MC4100 + *SitA-lacZ* fusion + (C12A)Mur_{Rl}	46 ± 16	151 ± 15

RESULTS

A (C12A)Mur_{Rl} Mutant Has Similar Properties to the Wild-Type Protein in Vivo. A single cysteine residue is found at position 12 in the sequence of Mur_{Rl} (Figure 2). Cysteine is also found at the corresponding position in the sequences of Fur_{Bj} and Zur_{Ec}, whereas in other Fur-like proteins, it is usually a leucine. *In vitro*, apoMur_{Rl} will, over time, form an intramolecular disulfide bridge, and the disulfide-bridged dimer loses its DNA-binding activity (manuscript in preparation). However, the addition of a suitable reductant such as DTT will break these bonds restoring activity. Because not all of the analytical methods that we required are consistent with the presence of reductants, we engineered an alanine mutant of the protein and tested its activity *in vivo* using a reporter plasmid containing the *sitABCD* promoter region as a fusion with *lacZ*. The results showed no significant difference between the wild type and the alanine mutant (Table 1). We also checked the folding of the mutant by CD analysis, which revealed very similar secondary-structure contents for the C12A mutant and wild-type Mur_{Rl}. We therefore concluded that (C12A)Mur_{Rl} can be used as a functional and structural substitute for the wild-type protein where necessary.

The Affinity of Binding of Mn(II) by (C12A)Mur_{Rl} in Vitro Is Higher Than for Other Transition Metals. ITC is one such method that does not allow for the presence of a reductant. Therefore, (C12A)Mur_{Rl} was used in quantitation of metal-binding affinities. Accordingly, ITC analysis showed two Mn(II) ions to bind to a (C12A)Mur_{Rl} dimer with the same individual dissociation constants (K_d of approximately 3.7 μM) within experimental error (Figure 3 and Table 2). No evidence for the occupation of further binding sites was observed up to a 10-fold molar excess of metal ion to protein monomer. This binding analysis was repeated for a number of other first-row divalent transition-metal cations including Fe(II), Co(II), Zn(II), and Ni(II). No binding was observed

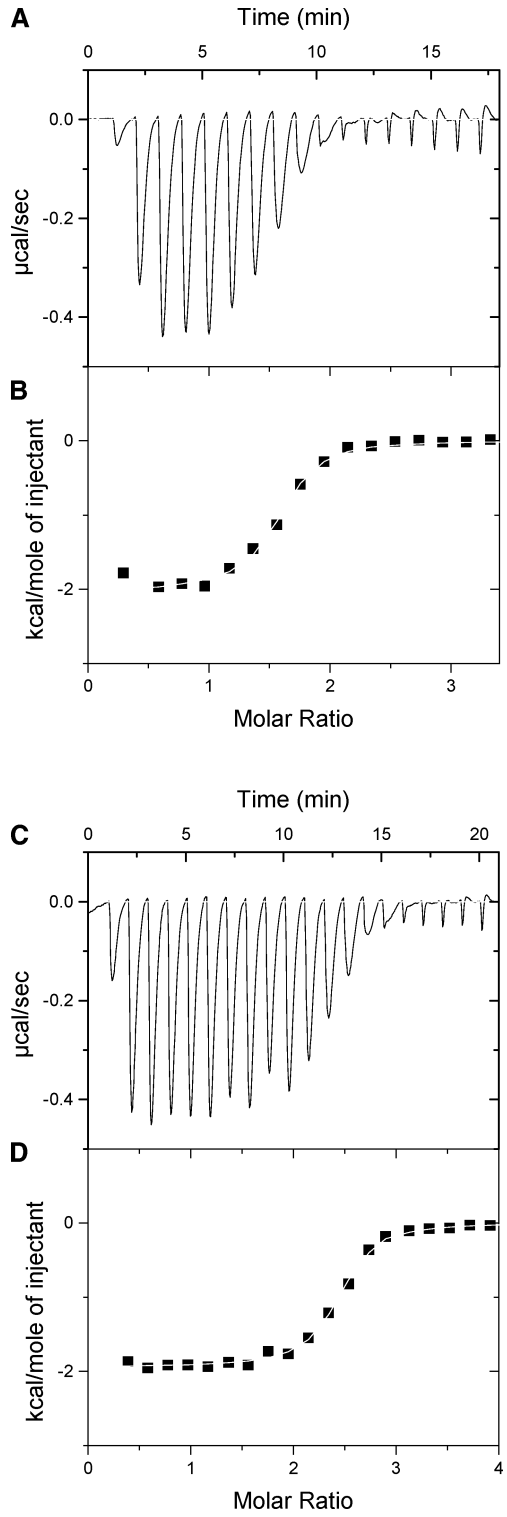

FIGURE 3: ITC analysis of apo(C12A)Mur_{Rl} titrated with Mn(II) and Fe(II). Raw data collection trace for titration of Mn(II) to a sample of (C12A)Mur_{Rl} and subsequent data analysis are shown as A and B, respectively. Similar data for the titration using Fe(II) are shown as C and D.

for the negative control, Ca(II). The results showed (C12A)-Mur_{Rl} to have the highest affinity for Mn(II) among the metals tested (Table 2). Of the remainder, (C12A)Mur_{Rl} showed similar, weaker affinities for Fe(II), Zn(II), and Co-(II), whereas Ni(II) was the least tightly bound. As was the case for Mn(II), no further metal-binding events were observed for any of the metal ions tested. The binding

Table 2: ITC-Derived Binding Affinities of (C12A)Mur_{Rl} for Different Transition Metals[a]

metal ion	N_1	K_{d_1} (μM)	N_2	K_{d_2} (μM)	R^2
Mn(II)	1.1 ± 0.05	3.6 ± 0.15	1.2 ± 0.1	3.8 ± 0.1	0.99
Fe(II)	1.0 ± 0.10	5.9 ± 0.4	1.0 ± 0.15	6.1 ± 0.1	0.99
Zn(II)	1.2 ± 0.2	11.5 ± 1.2	1.2 ± 0.1	12.7 ± 0.9	0.95
Co(II)	1.1 ± 0.2	5.3 ± 0.15	1.1 ± 0.1	5.8 ± 0.2	0.99
Ni(II)	1.20 ± 0.15	210 ± 35	1.15 ± 0.1	220 ± 25	0.95

[a] The results are based on a two-binding-site model fitted to titration data taken in triplicate. The calculated number of sites (N) and dissociation constant (K_d) are shown for each site. R^2 shows the goodness of fit.

Table 3: Observed and Calculated Molar Ratios of Metal Ions Bound Per Monomer of (C12A)Mur_{Rl} Following Dialysis[a]

dialysis metal	[Mn(II)] (μM)	[Zn(II)] (μM)	observed Mn(II) molar ratio (calculated)	observed Zn(II) molar ratio (calculated)
none	0.1 ± 0.0	0.1 ± 0.0		
Mn(II)	0.6 ± 0.1	0.1 ± 0.0	0.12 ± 0.02 (0.11)	0.02 ± 0.0
Zn(II)	0.1 ± 0.0	0.2 ± 0.1	0.02 ± 0.0	0.04 ± 0.02 (0.04)

[a] Protein samples were dialyzed against buffers containing either no metal ("none"), Mn(II), or Zn(II) followed by dialysis against metal-free buffer. Residual Mn(II) and Zn(II) concentrations were measured by ICP-AES, and observed molar ratios were derived from the known protein concentration. Calculated molar ratios (in parentheses) were derived using the metal-specific dissociation constants resulting from ITC analysis (see the Supporting Information for the method).

affinities of Mur_{Rl} for Mn(II) and Fe(II) measured in this study are slightly greater than those reported previously for Fur proteins. For example, Fur_{Ec} was reported to bind Fe(II) and Mn(II) with dissociation constants of 10 and 80 μM, respectively, by Bagg and Neilands (*32*) and 55 and 85 μM, respectively, by Hamed (*33*).

Mur_{Rl} Does Not Possess a Structural Zn(II) Binding Site. ITC results provided the first indication that the Mur_{Rl} dimer binds divalent cations at a ratio of two per dimer. We sought to confirm this using atomic emission spectroscopy. ICP-AES analysis of (C12A)Mur_{Rl} treated with either Mn(II) or Zn(II) and then dialyzed against metal-free buffer solutions showed a molar ratio of the metal ion to monomer of approximately 0.12 and 0.04 for Mn(II) and Zn(II), respectively (Table 3). If the two binding sites are really identical with a (mean) K_d value of 3.7 μM as the ITC results appear to suggest, then the amount of bound metal observed by ICP-AES should be predictable (see the Supporting Information). Note that this analysis assumes that the metal-binding sites are independent (no cooperativity). Using this approach, the predicted molar ratios for both Mn(II) or Zn(II) are in very good agreement with the experimental data (Table 3). Importantly, the accurate prediction of the molar ratios of bound metal ions observed by ICP-AES has provided an independent check on the accuracy of the binding affinities for Mn(II) and Zn(II) derived from ITC. The Donnan effect is the extra osmotic pressure of protein solutions caused by impermeable protein molecules resulting in the uneven distribution of small, permeant cations and anions in dialysis compartments. This causes an accumulation of charged permeable molecules on the side containing the charged proteins. This potential difference across the dialysis membrane is termed the Donnan potential. This phenomenon can affect the determination of an accurate dissociation constant

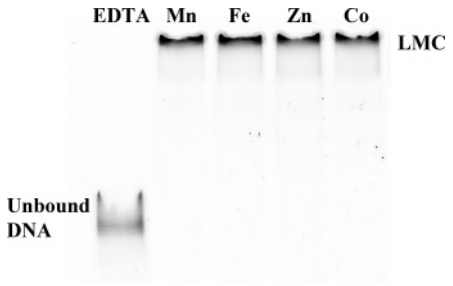

FIGURE 4: EMSA analysis of Mur_{Rl} binding to *mrs2* in the presence of various transition-metal ions. Samples contained 40 nM fluorescein-labeled *mrs2* dsDNA preincubated in binding reactions with 500 nM apoMur_{Rl} containing EDTA (apoprotein), Mn(II), Fe(II), Zn-(II), or Co(II) in 5-fold molar excess over the protein dimer concentration. A single LMC is formed in the presence of metal and the absence of EDTA.

in dialysis binding studies of, for example, metal−protein complexes. In the present study, however, this problem appears to have been overcome by use of 100 mM NaCl in the dialysis reservoir.

These results prove the absence of any tightly bound structural Zn(II) ion in Mur_{Rl}. Structural zinc ions bind at the S2 and S3 (when present) sites in other Fur proteins. The latter, high-affinity S3 site, which has been found in Fur_{Ec} and Fur_{Va}, can only be stripped of metal by denaturation of the protein and treatment with EDTA. The absence of an S3 metal ion in Mur_{Rl} is expected as the two cysteine residues that have been implicated in the binding of this zinc ion are absent in the Mur_{Rl} sequence (Figure 2). A comparison of the amino acid sequences of Mur_{Rl} and Fur_{Pa} shows that the residues contributing to S2 are conserved. Replacement of these residues by alanines in Fur_{Bj} did not effect the regulatory activity of the protein *in vitro* (*25*). It therefore appears that both of these rhizobial proteins may lack a functional S2 site.

Binding of Mur_{Rl} to mur Box dsDNA Is Independent of the Corepressor and Abolished in the Presence of EDTA. A number of EMSA experiments were performed containing 40 nM fluorescein-labeled *mrs2* dsDNA preincubated with 500 nM apoMur_{Rl} and each of the transition-metal ions Mn-(II), Fe(II), Zn(II), and Co(II). A 5-fold excess of metal ions over the protein dimer concentration was employed. To test the metal dependence of binding, a control experiment was performed in the presence of an equivalent concentration of EDTA added to the apo protein. In the presence of this excess of protein over dsDNA, a single band was observed for each metal employed (labeled as LMC in Figure 4). No retardation of dsDNA was evident in the absence of metal, i.e., in the EDTA-containing EMSA experiment. Thus, Mur_{Rl} requires bound metal to recognize and bind *mur* box DNA, but this binding will take place in the presence of not only Mn(II) but also Fe(II), Zn(II), and Co(II). Furthermore, no binding was observed to a negative control DNA probe, a fluorescein-labeled scrambled *fur* box, in the presence of any of the metals employed (results not shown).

Mur_{Rl} Forms a HMC and a LMC with both mur and fur Boxes in a Concentration-Dependent Manner. EMSA of Mur_{Rl} binding to *mrs1*, *mrs2*, to the *B. japonicum irr* promoter and to a canonical *fur* box showed the formation of two complexes: a HMC and a LMC formed at low and high protein concentrations, respectively. Figure 6 shows the results for gels run in the presence of Mn(II) and Fe(II). This phenomenon was observed to be independent of the metal used [except for Ca(II), the negative control, where no binding took place]. Determination of the molecular masses of the HMC and LMC by means of Ferguson plots revealed that in each case the HMC was due to one Mur_{Rl} dimer binding to DNA and the LMC was due to the binding of two Mur_{Rl} dimers. Baichoo and Helmann (*23*) demonstrated similar results for Fur_{Bs} binding to its cognate operator sequence, and Friedman and O'Brian (*19*) demonstrated similar results for the binding of Fur_{Bj} to the *B. japonicum irr* promoter region and to a canonical *fur* box. Our results demonstrate for the first time that Mur proteins bind to regulatory sequences in a fashion similar to that observed for other members of the superfamily.

No Cooperativity Is Observed in the Binding of Two Mur_{Rl} Dimers to a Canonical fur Box. To analyze the binding of Mur_{RL} to *fur* box DNA, it was first necessary to derive a new analytical relationship because standard methods are not valid when, as here, the protein concentration is not much greater than that of the DNA in the EMSAs. Importantly, also no analytical data is available in the literature specifying accurate K_d values for the binding of one and then two copies of a Fur superfamily dimer to a *fur* box-containing DNA duplex.

The cooperativity in the binding of two Mur_{Rl} binding dimers to a canonical *fur* box (considered as a bivalent receptor with two identical binding sites because of its palindromic nature) was assessed by separately fitting eqs 14, 15, and 16 to fractions of bound ligand in the LMC (y_2), in the HMC ($y_1 - y_2$), and in both ($y_1 + y_2$), measured as a function of the Mur_{Rl} concentration in the EMSA (Figure 5). These analyses, while not strictly independent, are subject to different experimental error and thus provide a useful internal check for consistency. Because K_{d_1} and K_{d_2} were found to be identical within experimental error (Table 4), we conclude that there is no cooperativity in binding.

Two Mur_{Rl} Dimers Bind with Different Affinities to Nonpalindromic Regulatory Sequences. Quantitative analysis of the binding of Mur_{Rl} to *mrs1* and *mrs2* proceeded as the interaction of the protein with bivalent receptors having nonidentical binding sites, assumed because of the differences in the sequences of the binding elements. The analysis was performed using eq 18 (parts i and ii in Figure 6). The fit to the experimental data (Table 5) was excellent, providing justification for the analytical model. In both cases, Mur_{Rl} was seen to bind with higher affinity to one of the two binding elements and with lower affinity to the other (Table 5). For example, in the case of the Mur_{Rl}−*mrs2* complex in the presence of excess Mn(II), K_d values of approximately 1 and 25 nM were observed. There was no major difference in the measured K_{d_1} or K_{d_2} values when measured in the presence of excess Mn(II) or Fe(II). This is the first report of the dissociation constant for the weaker-binding dimer of a Fur-like protein to a cognate operator sequence. While previous reports have presented only an overall effective binding constant for the sequential binding of two dimers, we note that, if K_{d_1} is much lower than K_{d_2}, then these previous analyses should yield relatively accurate estimates for the dissociation constant of the stronger dimer-binding site.

The same analysis was performed to quantify the affinity of Mur_{Rl} for the noncanonical *fur* box in the *B. japonocum*

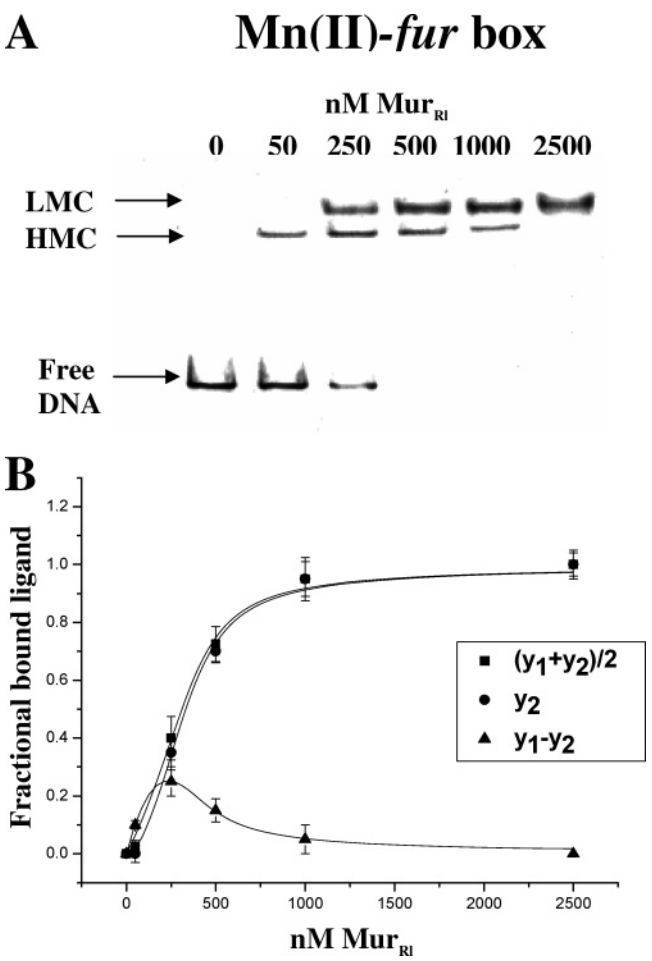

FIGURE 5: EMSA analysis of cooperativity in the binding of two Mur_{Rl} dimers to a canonical *fur* box in the presence of Mn(II). (A) 200 nM fluorescein-labeled canonical *fur* box dsDNA was titrated with increasing concentrations of Mur_{Rl} in binding reactions in the presence of Mn(II). Complexes were resolved on 12% nondenaturing polyacrylamide gels and visualized by fluorescence detection. The HMC, LMC, and unbound DNA are shown by arrows. (B) Relative fractions of LMC, HMC, and their sum were fitted to eqs 14, 15, and 16, respectively, to determine individual dissociation constants for the first and second binding Mur_{Rl} dimer.

Table 4: Comparison of the Binding Affinities of Mur_{Rl} for a Canonical *fur* Box in the Presence of Mn(II)[a]

Mur_{Rl}−*fur* box complex	K_{d_1} (nM)	K_{d_2} (nM)	R^2
LMC	36 ± 11	32 ± 8	0.99
HMC	36 ± 5	37 ± 4	0.99
HMC + LMC	34 ± 8	42 ± 11	0.99

[a] Derived from eqs 14, 15, and 16 using the observed fractions of the LMC, HMC, and their sum, respectively, in an EMSA. Fractional compositions of the high and low mobility complexes and their sum were derived by integration of fluorescence on a scanned EMSA gel. Data were used with the appropriate equation to derive estimates for the two dissociation constants, K_{d_1} and K_{d_2}. In the absence of error, each equation should report the same estimate for each of the two dissociation constants. R^2 reports the goodness of fit based on triplicate data points.

irr promoter (part iii in Figure 6). This showed that Mur_{Rl} binds more weakly to this operator than to its cognate *mur* boxes. It has an approximately 10−30-fold higher K_{d_1} and 10-fold higher K_{d_2} with this promoter than observed with *mrs1* and *mrs2* (Table 5). On the other hand, the first Mur_{Rl} dimer binds with approximately the same affinity to this promoter region as to a canonical *fur* box, whereas the affinity estimated for the second binding event is approximately 4-fold higher.

Note that with a binding analysis such as this, in the case for which the two binding sites are nonidentical, it is not possible to unambiguously distinguish whether the difference between K_{d_1} and K_{d_2} is due to negative cooperativity or simply a difference in the structure of the binding elements. However, in the case of a canonical *fur* box, for which it is possible to determine the degree of cooperativity because the regulatory sequence is composed of two identical binding elements, no cooperativity was detected. Therefore, it is arguably true that the results presented in Table 5 more likely reflect the fact that the two binding elements within each sequence are independent and that K_{d_2} is higher than K_{d_1} in these cases merely because of the structural differences between the two binding elements.

The Affinity of Mur_{Rl} for dsDNA Containing mrs2 and fur Boxes in Vitro Is Independent of the Corepressor. Other Fur proteins such as Fur_{Ec} and Fur_{Va} have been shown to bind to dsDNA *in vitro* in the presence of various divalent metals (*27*, *30*, *32*), and we had already seen that Mur_{Rl} was activated by a variety of metal ions for binding to *mrs2* (Figure 4). The EMSA analyses described above were therefore repeated in the presence of Fe(II) in place of Mn(II) to quantify the affinity of the interaction. In each case, no significant difference was observed (Table 5 and Figure 6). This was an unexpected result because it has been reported that *in vivo* Mur_{Rl} recognizes *mur* boxes in response to Mn(II) and *fur* boxes in response to Fe(II) (*15*). Given this result, we were interested to also quantify the affinities of Mur_{Rl} for a *mur* box in the presence of further divalent metal cations. Mur_{Rl} was found to bind to both *mrs2* and a canonical *fur* box *in vitro* with approximately the same K_{d_1} and K_{d_2} in the presence of Mn(II), Fe(II), Zn(II), or Co(II) (Tables 5 and 6 and Figure 7). It appears that the precise nature of the coordination geometry at the sensing sites in Mur_{Rl} once occupied does not influence the interaction of the protein with DNA.

DISCUSSION

Metalloregulatory proteins serve as a direct link between intracellular metal ion levels and the expression of metal-specific uptake, efflux, and storage systems (*34*). In general, metal ions bind in a reversible fashion to a sensing site in the regulator. This in turn leads to a change in the conformation (activation) of the regulator, which can direct changes in gene expression. The intracellular concentration of freely exchangeable metal ions is determined by the relative affinities of the sensing (regulatory) site for different metal ions. High selectivity (discrimination) at this site for the target metal(s) from the set of those present is required to ensure that the remainder do not interfere with its regulatory activity.

The regulatory ion-binding (sensing) sites of metalloregulatory sensor proteins should have affinities that are suitable for rapid, reversible uptake of the target metal ion. This appears to be the case for the Fur protein of *E. coli*, which has been shown to bind Fe(II) with a dissociation constant of micromolar order (*32*, *33*). We have now shown that the *R. leguminosarum* manganese uptake regulator binds Mn(II) with a similar absolute affinity. In the general case, the

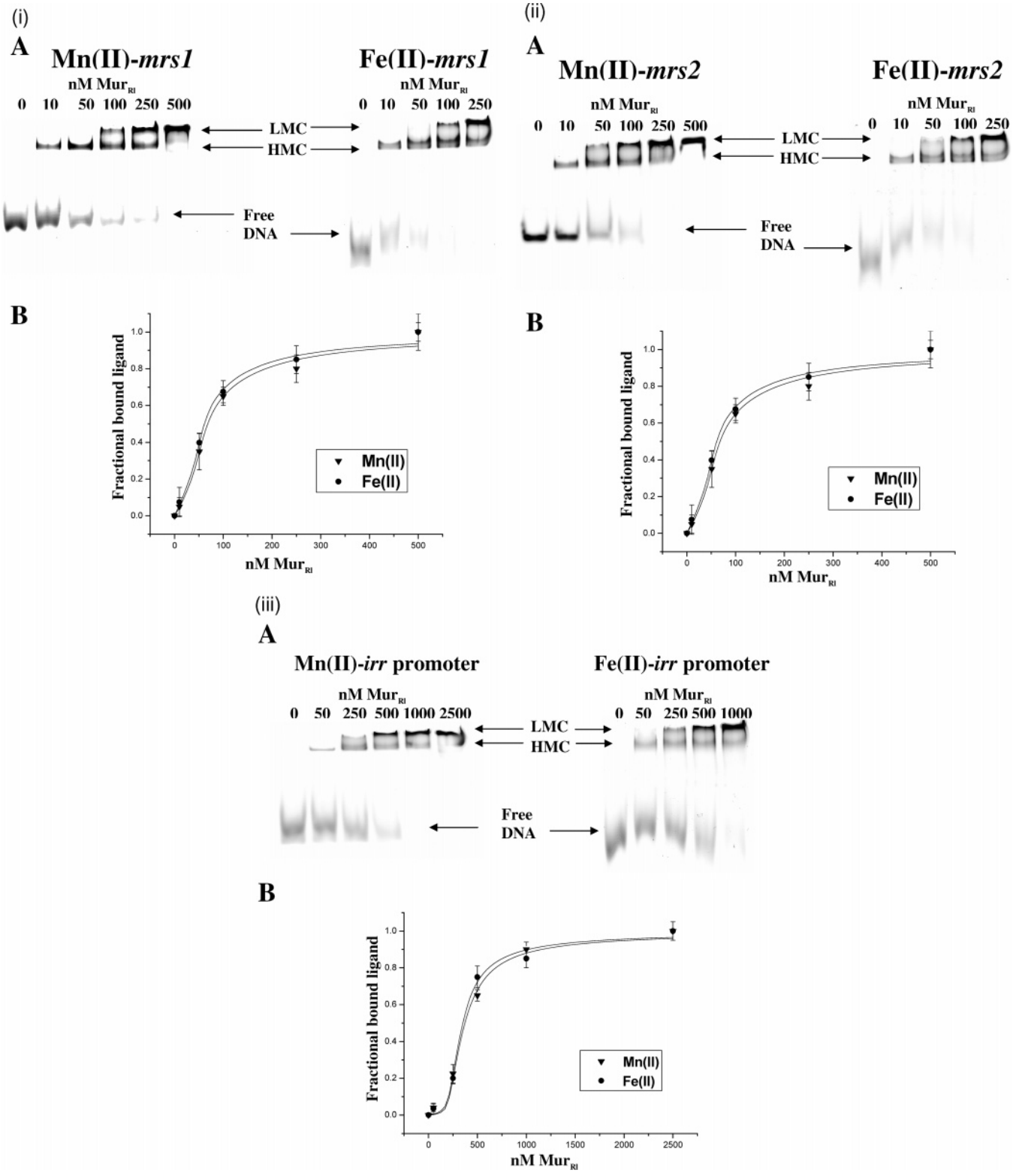

FIGURE 6: EMSA analysis of individual binding affinities of Mur_{RI} with regulatory sequence-derived DNA probes in the presence of either Mn(II) or Fe(II) (i) *mrs1*, (ii) *mrs2*, and (iii) *B. japonicum irr* promoter region. (A) Appropriate fluorescein-labeled dsDNA was titrated with increasing concentrations of Mur_{RI} in binding reactions in the presence of either Mn(II) or Fe(II). Complexes were resolved on 12% nondenaturing polyacrylamide gels and visualized as described in the Experimental Procedures. The HMC, LMC, and unbound DNA are shown by the arrows. (B) Data (relative fractions of HMC + 2×LMC) were fitted to eq 18 to determine individual dissociation constants for the first and second binding Mur_{RI} dimer in the presence of either Mn(II) or Fe(II).

nature of the residues contributing to the sensing site imparts selectivity by means of their specific coordination chemistry. However, Fur_{Ec} shows little or no selectivity for Fe(II) over Mn(II) or indeed Co(II) (*32*, *33*), allowing Mn(II) to be used as a surrogate corepressor in many studies. In fact, the low metal ion selectivity of Fur proteins has been used for the selection of Fur mutants as manganese-resistant mutants in different bacterial species (*35*). This lack of discrimination is also seen for Mur_{RI}, which binds Mn(II) only slightly more avidly than Fe(II), and this appears at first to be at odds with

Table 5: Comparison of the Binding Affinities of Mur_{Rl} for Various Regulatory Sequence-Based DNA Probes in the Presence of Mn(II) or Fe(II)[a]

box	metal ion	K_{d_1} (nM)	K_{d_2} (nM)	R^2
mrs1	Mn(II)	3.5 ± 1.4	72 ± 22	0.98
	Fe(II)	2.6 ± 0.7	55 ± 15	0.99
mrs2	Mn(II)	1.1 ± 0.4	25 ± 7	0.99
	Fe(II)	1.6 ± 0.7	35 ± 15	0.98
fur	Mn(II)	33 ± 10	40 ± 9	0.98
	Fe(II)	39 ± 12	45 ± 9	0.99
irr	Mn(II)	38 ± 12	142 ± 29	0.99
	Fe(II)	29 ± 6	121 ± 15	0.98

[a] Derived from eq 18. Fractional compositions calculated as the sum of the high and low mobility complexes were derived by integration of fluorescence as a function of the Mur_{Rl} concentration on a scanned EMSA gel. Data were applied to eq 18 to derive estimates for the two dissociation constants, K_{d_1} and K_{d_2}. R^2 reports the goodness of fit based on triplicate data points.

Table 6: Comparison of the Binding Affinities of Mur_{Rl} for *mrs2* and a Canonical *fur* Box in the Presence of Zn(II) or Co(II)[a]

metal ion	box	K_{d_1} (nM)	K_{d_2} (nM)	R^2
Zn(II)	*mrs2*	0.8 ± 0.3	20 ± 5	0.99
	fur	42 ± 7	33 ± 7	0.99
Co(II)	*mrs2*	0.9 ± 0.4	28 ± 6	0.98
	fur	40 ± 8	35 ± 6	0.99

[a] Derived from eq 18. Fractional compositions calculated as the sum of the high and low mobility complexes were derived by integration of fluorescence as a function of the Mur_{Rl} concentration on a scanned EMSA gel. Data were applied to eq 18 to derive estimates for the two dissociation constants, K_{d_1} and K_{d_2}. R^2 reports the goodness of fit based on triplicate data points.

the reported *in vivo* data (*15*). On the other hand, the features characterizing regulatory ion-binding sites are quite different from those of structural metal ion sites of metalloproteins. These are typically of high affinity, and the metal ion exchanges only slowly into the environment. All Fur superfamily proteins characterized to date, with the sole exception of Fur_{Bj} (*25*), are presumed to bind at least two metal ions per protein monomer. Using the nomenclature proposed by Pohl et al. (*24*), these would occupy the sensing (S1) site and the structural (S2) sites. A further high-affinity structural metal-binding site (the S3 site) is found in a subset of Fur proteins, such as Fur_{Ec} and Fur_{Va}, which possess specific cysteine residues in the C-terminal domain (Figure 2). Mur_{Rl} provides a further exception to this trend because it binds only two manganese ions per Mur_{Rl} dimer. This stoichiometry was also found for the other divalent metal ions tested, including Fe(II). We have also shown that this is the stoichiometry needed to activate the protein for binding to operator-based DNA fragments. In our EMSA experiments, we found that Mur_{Rl} retards both *mur*, *fur*, and *fur*-like box-containing DNA sequences in the presence of both Mn(II) and Fe(II). The measured affinities are, in all cases, independent of the actual metal used. Interestingly, Mur_{Rl} can also be activated by other transition-metal cations, including Zn(II) and Co(II), and binds to *mrs2* and a canonical *fur* box with affinities that are very similar to that observed for Mn(II). These findings suggest that a number of transition metals, when present at a sufficiently high concentration, can occupy the single sensing site per monomer, causing Mur_{Rl} to recognize regulatory sequences with the same (metal-independent) affinity. The data from

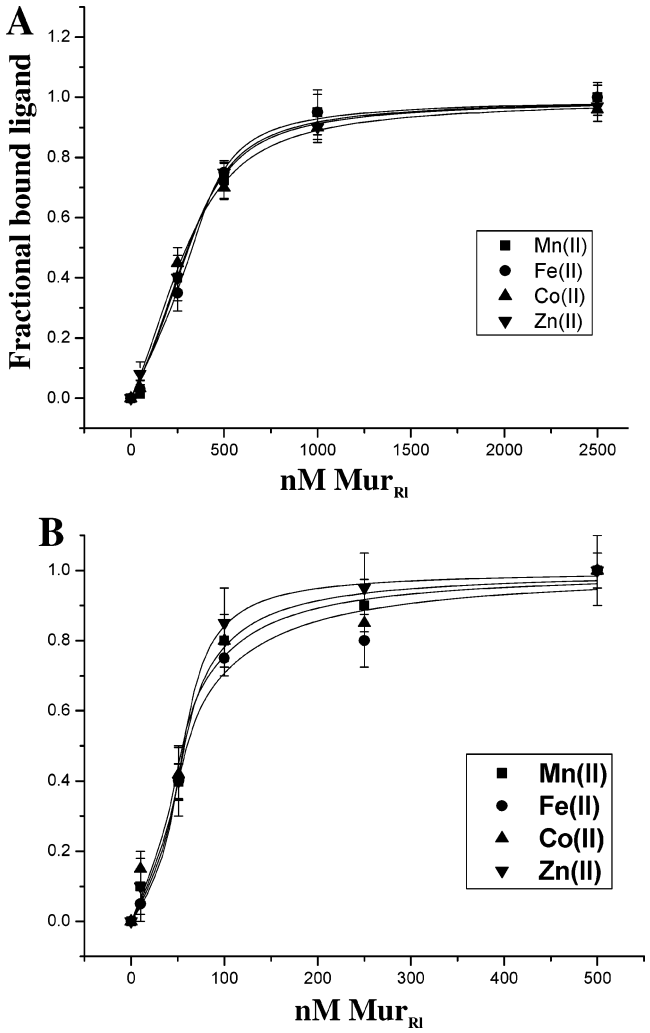

FIGURE 7: EMSA analysis of binding affinities of two Mur_{Rl} dimers to a canonical *fur* box and to *mrs2* in the presence of either Mn(II), Fe(II), Zn(II), or Co(II). The 200 nM fluorescein-labeled canonical *fur* box dsDNA or 40 nM fluorescein-labeled *mrs2* dsDNA were titrated with increasing concentrations of Mur_{Rl} in binding reactions in the presence of various transition metals (results not shown). Complexes were resolved on 12% nondenaturing polyacrylamide gels and visualized as described in the Experimental Procedures. The data (relative fractions of HMC + 2×LMC) were fitted to eq 18 to determine individual binding affinities for a canonical *fur* box (A) and *mrs2* (B) in the presence of different transition metals.

ITC, verified by equilibrium dialysis and atomic emission spectroscopy, show that two Mn(II) ions bind to apoMur_{Rl}. It follows that, unless additional metal-binding sites are generated in the Mur_{Rl}/DNA complex (which is possible, but we believe quite unlikely), only two manganese ions per protein dimer are required for activation.

In the holo-Fur_{Pa} structure solved from crystals grown at a high zinc ion concentration, zinc ions were observed to replace ferrous ions in the two structurally equivalent sensing sites, one in each monomer. In an ICP-AES analysis reported by Lewin et al. (*28*), Zn(II) ions were found at a ratio of 0.94 per Fur_{Pa} monomer. Using the dialysis conditions reported in that paper, we found that the reported molar ratio of Zn(II) is consistent with a dissociation constant of approximately 9 nM for Zn(II) binding to Fur_{Pa}. This result provides support for the presence of a high-affinity Zn(II) site in Fur_{Pa}, and we presume that this corresponds to the

S2 site as seen in the crystal structure. In the case of Mur_{Rl}, where we find a weaker affinity for Zn(II) in this work, it is more likely that Zn(II) binds at the Mn(II)-sensing site and there is no formal Zn(II)-binding structural site. A lack of a structural Zn(II) ion was also inferred by Friedman and O'Brian (*25*) in their studies of Fur_{Bj}, where replacement of the four putative Zn(II)-binding residues at the S2 locus by alanines did not affect the transcription repressional activity of the protein *in vitro*. Therefore, by direct analogy with Fur_{Bj}, we suggest that the sensing site in Mur_{Rl} corresponds to S1 as defined by Pohl et al. (*24*); however, this supposition has not been directly tested in this study, for example, by mutagenesis.

A number of alternative interpretations of the *fur* box sequence can be found in the literature. One recently aired view is that of a pair of overlapping (7−1−7) partially palindromic repeats consistent with the binding of a pair of dimers (*23*). This model is conceptually similar to that found in DtxR, which binds as a pair of dimers to its operator (the *tox* box), one to each repeat (*36*). In the present work, we have demonstrated that Mur_{Rl} can bind to various *fur*-like boxes as one and two homodimers with, in most cases, different individual dissociation constants K_{d_1} and K_{d_2}. We note at this point that, although we have used only short (27 bp) fluorescein-labeled DNA probes for these experiments, we believe that the binding affinities that we have derived will not differ significantly from those obtainable for longer DNA fragments. Our binding affinity analysis cannot provide definitive proof as to whether the differences in binding affinities within a DNA box are due to negative cooperativity or rather to the two binding elements having independent and possibly different affinities because of the differences in their nucleotide sequences. Both factors may also be operational. However, considering the fact that two Mur_{Rl} dimers bind to a canonical *fur* box (which has an essentially palindromic sequence and presumably, therefore, identical binding sites for the repressor protein) with identical dissociation constants K_{d_1} and K_{d_2} within experimental error, it appears that the affinity for a binding element in an operator sequence should not be affected by the occupation of the other binding element. It should therefore be possible, in cases in which one binding element in the operator sequence has an higher affinity than the other, to create novel operators with higher affinity by replacing the weaker binding element with a stronger one.

Because Mur_{Rl} can recognize a canonical *fur* box, it is not surprising that it is able to correct an *E. coli fur*$^-$ mutant (*17*). Why then does *R. leguminosarum* utilize a Mur protein, which is a functional Fur protein in *E. coli* at least, as a manganese uptake regulator and instead employ RirA and Irr to control iron homeostasis (*18*)? Although the dissociation constants of Fur_{Ec} and Mur_{Rl} for the transition metals that we tested are almost identical, these proteins can still apparently regulate Fe(II)-responsive genes in *E. coli* because the intracellular concentration of free Fe(II) has been reported to be approximately 10 μM and much higher than that of free Mn(II), Co(II), and Zn(II) (*32*, *37*). Unless the opposite balance of free Fe(II) and Mn(II) concentrations exists in *R. leguminosarum*, it is difficult to see, on the basis of the knowledge of dissociation constants alone, how Mur_{Rl} can act selectively as a manganese uptake regulator unless other mechanisms are operational. The simplest explanation would be that the intracellular concentration of Mn(II) is significantly higher than that of Fe(II) in *R. leguminosarum*, although this remains to be verified experimentally. In light of these considerations, we suggest that the selectivity of the metal-sensing site in the Fur-like protein, Mur_{Rl}, of *R. leguminosarum* may be insufficient to ensure high fidelity regulation of iron homeostasis mechanisms and therefore alternative regulators are employed. These considerations may also be extended to other α proteobacteria where Mur proteins are found but not Fur proteins nor canonical *fur* boxes, such as *S. meliloti*.

ACKNOWLEDGMENT

We thank Dr. G. J. Daniels for bringing to our attention the existence of an analytical solution for a cubic equation, Liz Rix for ICP-AES analysis, and Anne Reilly for help with gel-filtration chromatography. We are also indebted to Andrew Johnston for gift of a *sitABCD* promoter-*lacZ* reporter fusion plasmid.

SUPPORTING INFORMATION AVAILABLE

(1) Prediction of the concentration of the protein−ligand complex formed during dialysis. The method used to predict the concentration of a metal ion present in a protein sample once dialysis has reached equilibrium using known values of K_d (in this case derived from ITC experiments) and binding-site concentration. (2) Determination of the stoichiometry of binding for the Mur_{Rl} interaction with a *mur* box. This material is available free of charge via the Internet at http://pubs.acs.org.

REFERENCES

1. Hantke, K. (2001) Iron and metal regulation in bacteria, *Curr. Opin. Microbiol. 4*, 172−177.
2. McHugh, J. P., Rodriguez-Quinones, F., Abdul-Tehrani, H., Svistunenko, D. A., Poole, R. K., Cooper, C. E., and Andrews, S. C. (2003) Global iron-dependent gene regulation in *Escherichia coli*. A new mechanism for iron homeostasis, *J. Biol. Chem. 278*, 29478−29486.
3. Gaballa, A., and Helmann, J. D. (1998) Identification of a zinc-specific metalloregulatory protein, Zur, controlling zinc transport operons in *Bacillus subtilis*, *J. Bacteriol. 180*, 5815−5821.
4. Patzer, S. I., and Hantke, K. (1998) The ZnuABC high-affinity zinc uptake system and its regulator Zur in *Escherichia coli*, *Mol. Microbiol. 28*, 1199−1210.
5. Dalet, K., Gouin, E., Cenatiempo, Y., Cossart, P., and Hechard, Y. (1999) Characterisation of a new operon encoding a Zur-like protein and an associated ABC zinc permease in *Listeria monocytogenes*, *FEMS Microbiol. Lett. 174*, 111−116.
6. Bsat, N., Herbig, A., Casillas-Martinez, L., Setlow, P., and Helmann, J. D. (1998) *Bacillus subtilis* contains multiple Fur homologues: Identification of the iron uptake (Fur) and peroxide regulon (PerR) repressors, *Mol. Microbiol. 29*, 189−198.
7. van Vliet, A. H., Baillon, M. L., Penn, C. W., and Ketley, J. M. (1999) *Campylobacter jejuni* contains two fur homologs: Characterization of iron-responsive regulation of peroxide stress defense genes by the PerR repressor, *J. Bacteriol. 181*, 6371−6376.
8. Horsburgh, M. J., Clements, M. O., Crossley, H., Ingham, E., and Foster, S. J. (2001) PerR controls oxidative stress resistance and iron storage proteins and is required for virulence in *Staphylococcus aureus*, *Infect. Immun. 69*, 3744−3754.
9. Ricci, S., Janulczyk, R., and Bjorck, L. (2002) The regulator PerR is involved in oxidative stress response and iron homeostasis and is necessary for full virulence of *Streptococcus pyogenes*, *Infect. Immun. 70*, 4968−4976.
10. Fuangthong, M., Herbig, A. F., Bsat, N., and Helmann, J. D. (2002) Regulation of the *Bacillus subtilis* fur and perR genes by PerR: Not all members of the PerR regulon are peroxide inducible, *J. Bacteriol. 184*, 3276−3286.

11. Hamza, I., Chauhan, S., Hassett, R., and O'Brian, M. R. (1998) The bacterial irr protein is required for coordination of heme biosynthesis with iron availability, *J. Biol. Chem. 273*, 21669−21674.
12. Qi, Z., Hamza, I., and O'Brian, M. R. (1999) Heme is an effector molecule for irondependent degradation of the bacterial iron response regulator (Irr) protein, *Proc. Natl. Acad. Sci. U.S.A. 96*, 13056−13061.
13. Bearden, S. W., and Perry, R. D. (1999) The Yfe system of *Yersinia pestis* transports iron and manganese and is required for full virulence of plague, *Mol. Microbiol. 32*, 403−414.
14. Kehres, D. G., Janakiraman, A., Slauch, J. M., and Maguire, M. E. (2002) Regulation of *Salmonella enterica* serovar Typhimurium mntH transcription by H_2O_2, Fe^{2+}, and Mn^{2+}, *J. Bacteriol. 184*, 3151−3158.
15. Díaz-Mireles, E., Wexler, M., Sawers, G., Bellini, D., Todd, J. D., and Johnston, A. W. B. (2004) The Fur-like protein Mur of *Rhizobium leguminosarum* is a Mn^{2+}-responsive transcriptional regulator, *Microbiology 150*, 1447−1456.
16. Platero, R., Peixoto, L., O'Brian, M. R., and Fabiano, E. (2004) Fur is involved in manganese-dependent regulation of *mntA* (*sitA*) expression in *Sinorhizobium meliloti*, *Appl. Environ. Microbiol. 70*, 4349−4355.
17. Wexler, M., Todd, J. D., Kolade, O., Bellini, D., Hemmings, A. M., Sawers, G., and Johnston, A. W. B. (2003) Fur is not the global regulator of iron uptake genes in *Rhizobium leguminosarum*, *Microbiology 149*, 1357−1365.
18. Todd, J. D., Wexler, M., Sawers, G., Yeoman, K. H., Poole, P. S., and Johnston, A. W. B. (2002) RirA, an iron-responsive regulator in the symbiotic bacterium *Rhizobium leguminosarum*, *Microbiology 148*, 4059−4071.
19. Friedman, Y. E., and O'Brian, M. R. (2003) A novel DNA-binding site for the ferric uptake regulator (Fur) protein from *Bradyrhizobium japonicum*, *J. Biol. Chem. 278*, 38395−38401.
20. Hamza, I., Qi, Z., King, N. D., and O'Brian, M. R. (2000) Fur-independent regulation of iron metabolism by Irr in *Bradyrhizobium japonicum*, *Microbiology 146*, 669−676.
21. de Lorenzo, V., Wee, S., Herrero, M., and Neilands, J. B. (1987) Operator sequences of the aerobactin operon of plasmid ColV-K30 binding the ferric uptake regulation (fur) repressor, *J. Bacteriol. 169*, 2624−2630.
22. Escolar, L., Perez-Martin, J., and de Lorenzo, V. (1999) Opening the iron box: Transcriptional metalloregulation by the Fur protein, *J. Bacteriol. 181*, 6223−6229.
23. Baichoo, N., and Helmann, J. D. (2002) Recognition of DNA by Fur: A reinterpretation of the Fur box consensus sequence, *J. Bacteriol. 184*, 5826−5832.
24. Pohl, E., Haller, J. C., Mijovilovich, A., Meyer-Klaucke, W., Garman, E., and Vasil, M. L. (2003) Architecture of a protein central to iron homeostasis: Crystal structure and spectroscopic analysis of the ferric uptake regulator, *Mol. Microbiol. 47*, 903−915.
25. Friedman, Y. E., and O'Brian, M. R. (2004) The ferric uptake regulator (Fur) protein from *Bradyrhizobium japonicum* is an iron-responsive transcriptional repressor *in vitro*, *J. Biol. Chem. 279*, 32100−32105.
26. Jacquamet, L., Aberdam, D., Adrait, A., Hazemann, J., L., Latour, J., M., and Michaud-Soret, I. (1998) X-ray absorption spectroscopy of a new zinc site in the fur protein from *Escherichia coli*, *Biochemistry 37*, 2564−2571.
27. Zheleznova, E. E., Crosa, J. H., and Brennan, R. G. (2000) Characterization of the DNA- and metal-binding properties of *Vibrio anguillarum* fur reveals conservation of a structural Zn^{2+} ion, *J. Bacteriol. 182*, 6264−6267.
28. Lewin, A. C., Doughty, P. A., Flegg, L., Moore, G. R., and Spiro, S. (2002) The ferric uptake regulator of *Pseudomonas aeruginosa* has no essential cysteine residues and does not contain a structural zinc ion, *Microbiology 148*, 2449−2456.
29. Bohm, G., Muhr, R., and Jaenicke, R. (1992) Quantitative analysis of protein far UV circular dichroism spectra by neural networks, *Protein Eng. 5*, 191−195.
30. Ochsner, U. A., and Vasil, M. L. (1996) Gene repression by the ferric uptake regulator in *Pseudomonas aeruginosa*: Cycle selection of iron-regulated genes, *Proc. Natl. Acad. Sci. U.S.A. 93*, 4409−4414.
31. Klotz, I. M. (1997) *Ligand−Receptor Energetics: A Guide for the Perplexed*. John Wiley and Sons, New York.
32. Bagg, A., and Neilands, J. B. (1987) Ferric uptake regulation protein acts as a repressor, employing iron (II) as a cofactor to bind the operator of an iron transport operon in *Escherichia coli*, *Biochemistry 26*, 5471−5477.
33. Hamed, M. Y. (1993) Binding of the ferric uptake regulation repressor protein (Fur) to Mn(II), Fe(II), Co(II), and Cu(II) ions as co-repressors: Electronic absorption, equilibrium, and 57Fe Mossbauer studies, *J. Inorg. Biochem. 50*, 193−210. Erratum in: *J. Inorg. Biochem. 52*, 78.
34. O'Halloran, T. V. (1993) Transition metals in control of gene expression, *Science 261*, 715−725.
35. Hantke, K. (1987) Selection procedure for deregulated iron transport mutants (fur) in *Escherichia coli* K 12: fur not only affects iron metabolism, *Mol. Gen. Genet. 210*, 135−139.
36. White, A., Ding, X., van der Spek, J. C., Murphy, J. R., and Ringe, D. (1998) Structure of the metal-ion-activated diphtheria toxin repressor/tox operator complex, *Nature 394*, 502−506.
37. Keyer, K., and Imlay, J. A. (1996) Superoxide accelerates DNA damage by elevating free-iron levels, *Proc. Natl. Acad. Sci. U.S.A. 93*, 13635−13640.
38. Notredame, C., Higgins, D., and Heringa, J. (2000) T-Coffee: A novel method for multiple sequence alignments, *J. Mol. Biol. 302*, 205−217.

BI052081N